Am J Transl Res 2022;14(5):3407-3418
www.ajtr.org /ISSN:1943-8141/AJTR0143133

*Original Article*

# BMI1 governs the maintenance of mouse GC-2 cells through epigenetic repression of *Foxl1* transcription

Bo Zheng[1*], Juanjuan Liu[2*], Xiaodan Shi[3*], Jinfu Xu[4], Ke Zhang[5], Hui Zhou[6], Tiantian Wu[4], Xiaoyan Huang[4], Cong Shen[1], Yuting Liang[7], Dan Zhao[8], Yueshuai Guo[4]

*[1]State Key Laboratory of Reproductive Medicine, Center for Reproduction and Genetics, Suzhou Municipal Hospital, The Affiliated Suzhou Hospital of Nanjing Medical University, Gusu School, Nanjing Medical University, Suzhou 215002, Jiangsu, China; [2]Reproductive Medicine Center, The Second Affiliated Hospital of Soochow University, Suzhou 215004, Jiangsu, China; [3]Department of Reproduction, The Affiliated Obstetrics and Gynecology Hospital with Nanjing Medical University, Nanjing Maternity and Child Health Care Hospital, Nanjing 210004, Jiangsu, China; [4]State Key Laboratory of Reproductive Medicine, Department of Histology and Embryology, Nanjing Medical University, Nanjing 211166, Jiangsu, China; [5]Department of Urology, The Second Affiliated Hospital of Soochow University, Suzhou 215004, Jiangsu, China; [6]Human Reproductive and Genetic Center, Affiliated Hospital of Jiangnan University, Wuxi 214122, Jiangsu, China; [7]Center for Clinical Laboratory, The First Affiliated Hospital of Soochow University, Suzhou 215006, Jiangsu, China; [8]Fourth Affiliated Hospital of Jiangsu University, Zhenjiang 212008, Jiangsu, China. [*]Equal contributors.*

Received March 26, 2022; Accepted April 30, 2022; Epub May 15, 2022; Published May 30, 2022

**Abstract:** Objectives: Studies have demonstrated that B lymphoma Mo-MLV insertion region 1 (BMI1) plays an important role in male reproductive function and the regulation of spermatogonia proliferation. However, whether BMI1 exerts a similarly important function in spermatocyte development remains unclear. Methods: In this study, we investigated the role of BMI1 in spermatocyte development using a mouse spermatocyte-derived cell line (GC-2) and a *Bmi1*-knockout (KO) mouse model. Results: We demonstrated that BMI1 promoted the proliferation and inhibited the apoptosis of GC-2 cells. Mechanistically, we presented *in vitro* and *in vivo* evidence showing that BMI1 binds to the promoter region of the forkhead box L1 (*Foxl1*) gene, sequentially driving chromatin remodeling and gene silencing. BMI1, which functions as a classical polycomb protein, was found to direct the transcriptional repression of *Foxl1* through increasing the H2AK119ub level and reducing that of H3K4me3 in the promoter region of *Foxl1*. Our results further indicated that the knockdown of *Foxl1* expression significantly enhanced cell proliferation *via* activating β-catenin signaling in BMI1-deficient GC-2 cells. Conclusions: Collectively, our study revealed for the first time the existence of an epigenetic mechanism involving BMI1-mediated gene silencing in GC-2 cells development and provided potential targets for the treatment of male infertility.

**Keywords:** BMI1, spermatocyte, GC-2, Foxl1, β-catenin

## Introduction

Spermatogenesis is a unique and dynamic cellular proliferation and differentiation process that is mainly composed of three phases: self-renewal and differentiation of spermatogonia, spermiogenesis, and meiotic division of spermatocytes. Spermiogenesis must be rigorously managed to ensure that genetic and epigenetic information is transmitted correctly to the following generations [1]. The maintenance of this process is known to be precisely regulated *via* a complex multi-layered gene-protein network [2-4]; however, the mechanisms by which this regulation occurs remain unclear.

B lymphoma Mo-MLV insertion region 1 (BMI1) is a critical part of polycomb group (PcG) repressive complex 1 (PRC1) that represses gene expression by catalyzing and/or recognizing chromatin modifications [5]. BMI1 was first discovered to be an oncogene but was later discovered to be required for the proliferation of the cell, cell cycle regulation, and cell apoptosis [6-8]. We have previously reported that BMI1 is abundantly expressed in the testis of the mou-

se and is found in various testicular cell categories, including the germ and somatic cells [9]. Additionally, male infertility, reduction in the serum levels of testosterone, and disrupted spermatogenesis are observed in BMI1 knockout (KO) mice [9]. As an epigenetic inhibitor and antioxidant, BMI1 was finally discovered in primary Leydig cells and the mouse MLTC-1 Leydig cell line. Throughout preserving redox equilibrium and epigenetically suppressing the p38 MAPK signaling pathway, it was revealed by our results that BMI1 regulated steroidogenesis [10, 11]. In a subsequent investigation, through epigenetic regulation of the protein tyrosine phosphatase receptor type M (Ptprm) gene, we determined that BMI1 is required for the proliferation of a mouse spermatogonia cell line (GC-1) [12]. Nevertheless, the specific role of BMI1 in spermatocytes is unclear.

The forkhead box (FOX) protein superfamily is made up of multiple transcription factors that exhibit a remarkably conserved DNA-binding domain (forkhead/winged helix-box). Members of this protein family play crucial roles in the control of a diverse set of procedures during ontogenesis, including cell metabolism, proliferation, differentiation, and apoptosis [13]. Forkhead box L1 (FOXL1), a member of the FOXL protein subfamily, was first identified as a tumor suppressor [14-16]. Recent studies have implicated FOXL1 in the regulation of intestinal epithelial cell proliferation [17] and spermatogonial stem cell maintenance [12, 18]. Further mechanistic studies showed that the Wnt/β-catenin pathway is a major downstream target of FOXL1, mediating its regulatory effects in gut epithelia and tumor cell development [19, 20].

In this investigation, we explored the impact of BMI1 in mouse spermatocytes by the use of mouse spermatocyte-derived cell line (GC-2) and *Bmi1*-KO mice, as well as the regulatory mechanism underlying the BMI1-mediated regulation of the FOXL1/β-catenin signaling pathway.

## Materials and methods

### *Animals*

This work was authorized by the Welfare and Animal Ethical Committee of Nanjing Medical University (NO. 2004020). At Nanjing Medical University's Animal Center, mice were raised and kept in a pathogen-free environment. *Bmi1*-KO mice were obtained and genotyped as previously described [9].

### *Cell culture and reagents*

Through American Type Culture Collection (ATCC; Manassas, VA, USA; ATCC number: CRL-2196), the mouse spermatogenic cell line (GC-2) was obtained and cultured in a medium composed of high-glucose Dulbecco's modified Eagle's medium (DMEM; Gibco, Utah, CA, USA) and 10% fetal bovine serum (FBS; Thermo Scientific, Waltham, MA, USA). Cells were cultured in an incubator at 37°C with 5% $CO_2$. Lipofectamine 2000 reagent was used for transient transfection of small interfering RNA (siRNA) (Invitrogen, Carlsbad, CA, USA) according to the recommendations of the manufacturer. siRNAs targeting *Foxl1* (si-*Foxl1*-1: 5'-AUGCCGUUCAGUGUGACCC-3'; si-*Foxl1*-2: 5'-AAGCGUUGAAGGGAGGCGC-3') and negative control (NC) siRNA (si-NC; 5'-ACGUGACACGUUCGGAGAA-3') were provided by genePharma (Suzhou, China). PTC-209 was purchased from Selleck Chemicals, (Houston, TX, USA).

### *Western blotting*

Western blotting was carried out in the same manner as previously reported, with slight variations [21-23]. To summarise, radioimmunoprecipitation assay (RIPA) buffer was used to prepare cell lysates (Beyotime, Nantong, China). We used electro-transferred to polyvinylidene difluoride (PVDF) membranes and sodium dodecyl sulfate (SDS)-polyacrylamide gel electrophoresis (PAGE) to separate an equal amounts of extracted protein-(Bio-Rad, Hercules, CA, USA). After blocking in 5% (w/v) milk, the membranes were incubated overnight at 4°C with primary antibodies against BMI1 (1:2,000; Proteintech, Chicago, IL, USA) and tubulin (1:5,000; Beyotime), and then followed by washing for 2 hours at room temperature with horseradish peroxidase-conjugated secondary antibodies (Thermo Scientific). A chemiluminescent substrate was used to detect the signals (Thermo Scientific).

### *Flow cytometry*

For cell cycle analysis, before being fixed in cold ethanol overnight at 4°C, cells were rinsed three times with phosphate-buffered saline (PBS). The cells were resuspended in 0.5 mL of PBS and stained in the dark for 30 minutes with propidium iodide (PI) after rinsing two

times with PBS (BD Biosciences, Franklin Lakes, NJ, USA). A FACSCaliber flow cytometer was utilized to evaluate the samples (BD Biosciences).

*Cell proliferation*

The Cell Counting Kit-8 (CCK-8) (Beyotime) was used to measure cell viability, as previously reported [24]. After transfection with si-NC or si-*Foxl1* (both 50 nM) for 48 h, GC-2 cells were treated with CCK-8 solution (1:100 dilution) at the indicated time points for an additional 2 h. At 450 nm, absorbance was then evaluated.

GC-2 cells were seeded at 3,000 cells/well in six-well plates for the colony formation test and cultivated for two weeks, as previously reported [25]. Methanol was then used to fix the cells and stain them with crystal violet (Beyotime) according to the manufacturer's recommendations.

*Terminal deoxynucleotidyl transferase-dUTP nick-end labeling (TUNEL) assay*

Apoptotic cells were discovered using a TUNEL kit in compliance with the instructions of the manufacturer (Vazyme, Nanjing, China). Cells were preserved in 4% (w/v) PFA, permeabilized with 0.1% Triton X-100 for 10 minutes and then reacted for 1 hour at 37°C with BrightRed Labeling Mix. Following washing with PBS, a confocal laser scanning microscope was used to view and photograph the cells (LSM800, Carl Zeiss, Oberkochen, Germany).

*Immunofluorescence*

Cells were fixed in 4% PFA for 30 min, blocked in 1% bovine serum albumin at room temperature for 20 min, incubated first with antibody targeting BMI1 (1:200; Proteintech) or β-catenin (1:500; BD Biosciences) at 4°C overnight, and then with Alexa Fluor-conjugated secondary antibodies (Thermo Scientific) for 60 min at room temperature. Finally, the samples were stained with Hoechst (Beyotime), and a confocal microscope was utilized for imaging (Zeiss LSM800, Carl Zeiss).

*RNA isolation and real-time reverse transcription-quantitative PCR (RT-qPCR)*

Using the TRIzol reagent (Invitrogen), total RNA was extracted from GC-2 cells according to the recommendations of the manufacturer. A PrimeScript Reverse Transcription Kit was used to create cDNA (Vazyme). By the use of Applied Biosystems 7500 Real-time PCR system (Foster City, CA, USA), the relative expression of RNA transcripts was determined, with 18S rRNA acting as the internal reference. The sequences of the primers utilized were 5'-TGTTGTACGTGTACAGCCCC-3' (forward) and 5'-CGGGAAGCGATCCATGATGA-3' (reverse) for *Foxl1*. The sequences of the primers used for 18 s rRNA were as previously described [22].

*Immunoprecipitation and mass spectrometry*

GC-2 cells were lysed in RIPA buffer and incubated with anti-BMI1 antibody (Proteintech) at 4°C overnight. Invitrogen Protein A Dynabeads were collected by centrifugation and washed twice with PBS. SDS-PAGE were eluted with sample buffer containing 1% SDS and then used to separate the immune complexes after that. The gels were chopped into small pieces before being digested at 37°C overnight. As previously described, the digested peptides were evaluated using an Orbitrap Fusion Lumos mass spectrometer (Thermo Scientific) [12, 26]. The identified proteins are shown in Table S1.

*Chromatin immunoprecipitation (ChIP)*

Cells were collected and treated at room temperature for 10 min with a formaldehyde solution containing 1% formaldehyde for protein/DNA crosslinking. Using a Branson Sonifier, the cells were then sonicated to solubilize and shear the crosslinked DNA (Thermo Scientific). Anti-BMI1 antibodies were used to incubate the pre-cleared chromatin DNA-protein complexes (10 μg/ChIP; Proteintech), anti-H2AK119ub (10 μg/ChIP; Cell Signaling Technology), anti-Ring1B (10 μg/ChIP; Active Motif), and anti-H3K4me3 (5 μg/ChIP; Millipore) antibodies at 4°C overnight. For ChIP-qPCR analysis, we utilized the following primer sequences (forward and reverse, respectively): 5'-ACTAGCCCCGAAACCGATTG-3' and 5'-GTCCTTGTGTTCTCAGCCCA-3' for the *Foxl1* promoter; and 5'-AACCCAAACTAACAGTTGTCCCAA-3' and 5'-ACTCCTTGGAGGCCATGTAGG-3' for *Gapdh*.

*Statistical analysis*

Data are presented as mean ± SD. To evaluate significance, a two-tailed Student's t-test or

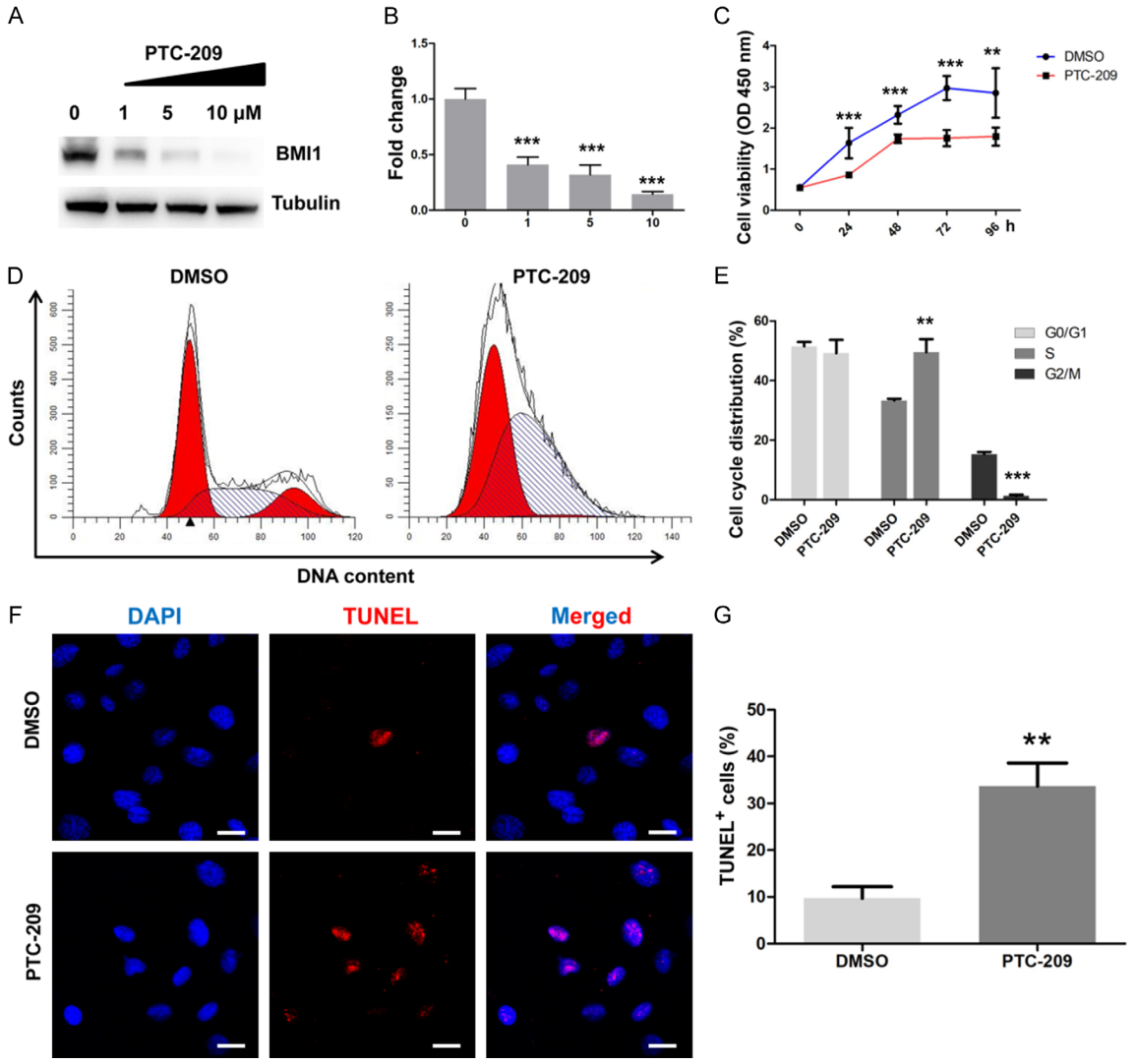


**Figure 1.** BMI1 is vital for GC-2 cell survival. (A) Western blotting of BMI1 expression in GC-2 cells treated with the indicated PTC-209 concentrations for 48 h. The experiments were repeated three times. (B) Quantification of (A). (C) Viability assay in GC-2 cells treated with PTC-209 (10 μM) or DMSO (control) for the indicated times. *n* = 6 for each group. (D) Flow cytometric analysis of the cell cycle in GC-2 cells treated with PTC-209 (10 μM) or DMSO (control) for 48 h. *n* = 3 for each group. (E) Quantification of (D). (F) TUNEL assay in GC-2 cells treated with PTC-209 (10 μM) or DMSO (control) for 48 h. *n* = 6 for each group. Scale bar: 20 μm. (G) Quantification of (F). For (B) data were analyzed using one-way ANOVA with Dunnett's post hoc test. For (C, E and G), data analysis was performed using the Student's two-tailed *t*-test. **P < 0.01, ***P < 0.001.

one-way ANOVA was utilized. *P*-values of < 0.05 were deemed significant.

## Results

### *Inhibition of BMI1 expression using PTC-209 treatment resulted in cell cycle arrest and increased rates of apoptosis*

PTC-209 was used to reduce BMI1 expression in GC-2 cells, and a BMI1-specific inhibitor was utilized [27, 28]. Three doses (1, 5, and 10 μM) of PTC-209 were used to treat GC-2 cells to test their inhibitory effectiveness in GC-1 mouse spermatogonia cells [12] and osteosarcoma cells [29]. As illustrated in **Figure 1A** and **1B**, PTC-209 treatment for 48 h resulted in a significant and concentration-dependent decrease in BMI1 levels. Consequently, PTC-209 treatment at 10 μM was used in the following studies. GC-2 cells treated with PTC-209 had lower viability after 24 hours compared to controls, which was demonstrated via the CCK-8 test (**Figure 1C**). Flow cytometric analysis dem-

onstrated that the fraction of PTC-209-treated GC-2 cells arrested in the S-phase increased significantly and a significant reduction in the numbers of those at the G2/M phase compared with that of dimethyl sulfoxide (DMSO)-treated control cells (**Figure 1D** and **1E**). In addition, TUNEL assay results revealed that PTC-209 treatment increased the rate of apoptosis in GC-2 cells (**Figure 1F** and **1G**). Overall, these results suggested that BMI1 can promote GC-2 cell proliferation and inhibit GC-2 cell apoptosis.

*BMI1 has the ability to suppress Foxl1 expression at the transcriptional level*

To explore BMI1's involvement in GC-2 cell survival, we first identified BMI1's subcellular location in GC-2 cells. Immunofluorescence staining showed that BMI1 was exclusively localized in the nucleus (**Figure 2A**). Subsequently, we undertook a proteomic analysis of immunoprecipitated BMI1 complexes in GC-2 cells (Table S1). Various components of PRC1 (Ring 1B, Cbx8, Ring 1A, Phc2, and Cbx7) have been found among the major candidate interactions (**Figure 2B**), strongly indicating that BMI1 functions as a polycomb protein in GC-2 cells. BMI1, together with the catalytic ring finger protein Ring1B, is required for PRC1 complex formation, orchestrating the monoubiquitination of histone H2A at lysine 119 (H2AK119ub). As a result, target gene expression is suppressed [30]. For this reason, we set out to find BMI1's direct targets in GC-2 cells. A strong BMI1 binding peak associated with the region of Foxl1 promoter was found via a bioinformatics study of publically available BMI1 ChIP-seq data for mouse germline stem cells [31] (**Figure 2C**). Further examination of the BMI1 peak revealed the presence of a functional motif, 5'-KCTGY-3', that was shown to be largely similar in rats, mice, monkeys, and humans (**Figure 2D**). The ChIP-qPCR results verified the BMI1 enrichment at the Foxl1 promoter area in GC-2 cells (**Figure 2E**). These results suggested that BMI1 can regulate GC-2 cell survival by targeting *Foxl1*. To confirm this possibility, we first assessed the *Foxl1* transcript levels and discovered that GC-2 cells treated with 10 M PTC-209 had considerably higher Foxl1 expression (**Figure 2F**). To learn more about the processes through which BMI1 regulates Foxl1 transcription, PTC-209 was used to reduce BMI1 expression in GC-2 cells and discovered a significant decrease in the amounts of H2AK119ub and Ring1B associated with the Foxl1 promoter region (**Figure 2G** and **2H**), suggesting that the function of PRC1 had been abrogated. H3K4me3 usually marks the transcriptional start site of the active genes [32] and directs the derepression of BMI1's targets [11]. Interestingly, The H3K4me3 level increased significantly in cells treated with PTC-209 (**Figure 2I**). Our findings show that BMI1 suppresses Foxl1 expression by assembling the PRC1 complex, which subsequently binds to the Foxl1 promoter area and modifies its chromatin accessibility.

*Foxl1 is involved in BMI1-mediated GC-2 cell growth*

To clarify the role of *Foxl1* in GC-2 cells, we downregulated *Foxl1* expression in these cells *via* treatment with either of two siRNAs (si-*Foxl1*-1 and si-*Foxl1*-2). Foxl1 expression was considerably lower in Foxl1-depleted cells compared to negative controls (si-NC-treated) (**Figure 3A**). Then, using CCK-8 tests, we investigated the impact of Foxl1 knockdown on cell viability and found that *Foxl1* knockdown significantly improved the viability of GC-2 cells relative to that seen in si-NC-treated cells (**Figure 3B**). We further analyzed the clonogenic ability of GC-2 cells using a colony formation assay and observed that *Foxl1*-depleted cells formed more colonies compared with si-NC treated cells (**Figure 3C** and **3D**). Collectively, these data showed that Foxl1 performs an inhibitory function in the development of GC-2 cells.

GC-2 cells were transfected with si-*Foxl1* and then treated with PTC-209 to further determine whether *Foxl1* is involved in BMI1-mediated GC-2 cell growth. We found that, compared with PTC-209 treatment alone, *Foxl1* knockdown in PTC-209-treated cells significantly improved the viability of GC-2 cells (**Figure 3E**) while relieving S-phase arrest (**Figure 3F** and **3G**) and reducing the levels of cell apoptosis (**Figure 3H** and **3I**). The above findings implied that *Foxl1* plays a major inhibitory role in BMI1-induced GC-2 cell growth.

The Wnt/β-catenin signaling pathway is well-known for being a critical regulator of cell proliferation, differentiation, fate, and apoptosis

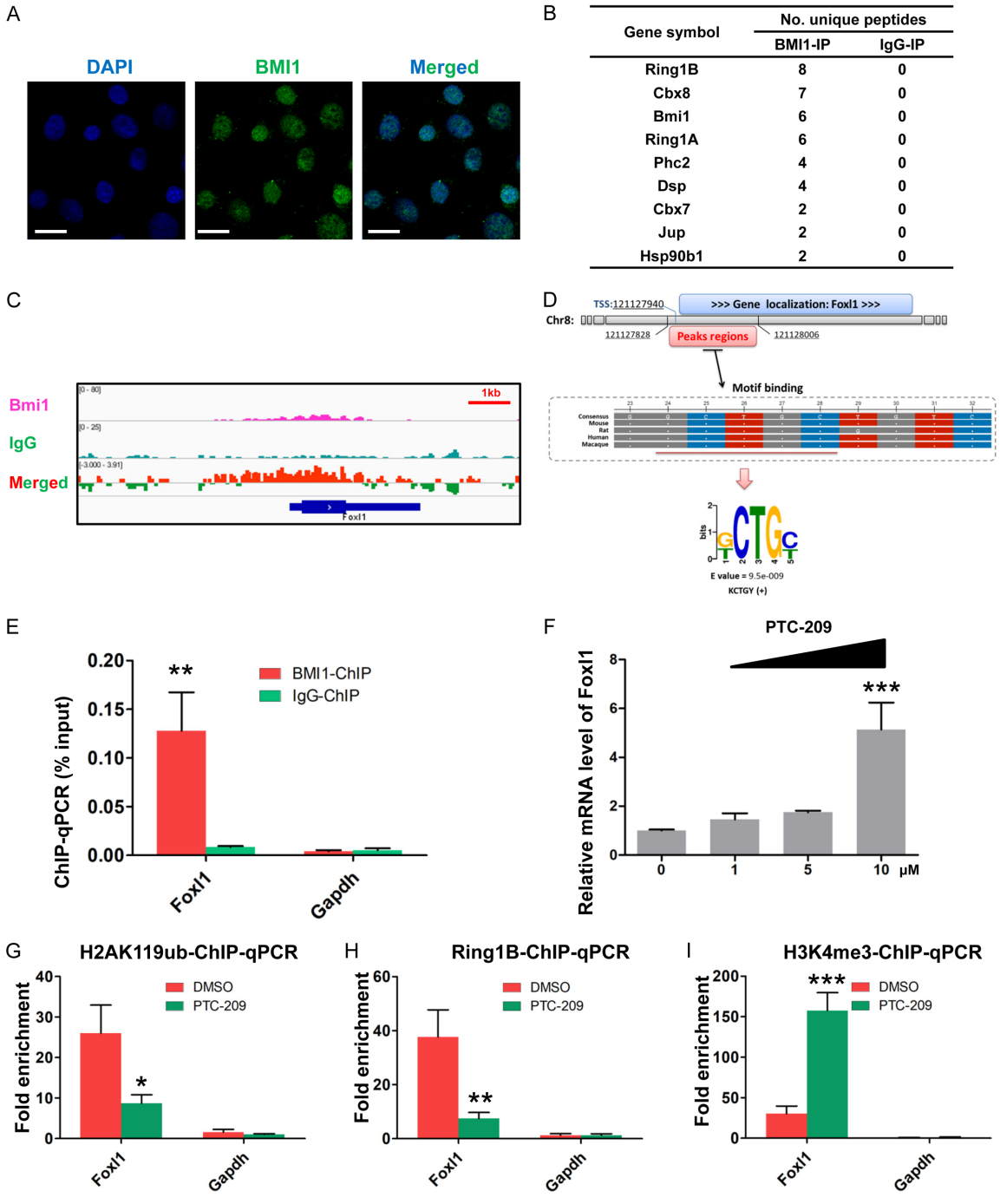


| Gene symbol | No. unique peptides | |
|---|---|---|
| | BMI1-IP | IgG-IP |
| Ring1B | 8 | 0 |
| Cbx8 | 7 | 0 |
| Bmi1 | 6 | 0 |
| Ring1A | 6 | 0 |
| Phc2 | 4 | 0 |
| Dsp | 4 | 0 |
| Cbx7 | 2 | 0 |
| Jup | 2 | 0 |
| Hsp90b1 | 2 | 0 |

**Figure 2.** BMI1 represses *Foxl1* transcription. (A) Immunofluorescence staining of BMI1 in GC-2 cells. The experiments were repeated three times. Scale bar: 20 μm. (B) Immunoprecipitation assay in GC-2 cells using an anti-BMI1 antibody. The precipitates were subjected to mass spectrometry for the identification of the interacting proteins. (C) The density of BMI1 ChIP-seq reads at *Foxl1* loci. (D) Sequence analysis of the BMI1 binding peak at the promoter region of *Foxl1*. (E) ChIP-qPCR for BMI1 distribution in the promoter region of *Foxl1* in GC-2 cells. *Gapdh* served as a negative control. $n = 3$ for each group. (F) RT-qPCR analysis of *Foxl1* expression in GC-2 cells treated with PTC-209 as indicated for 48 h. $n = 3$ for each group. (G-I) ChIP-qPCR for H2AK119ub (G), Ring1B (H), and H3K4me3 (I) distribution in the promoter region of *Foxl1* in GC-2 cells treated with PTC-209 (10 μM) or DMSO (control) for 48 h. The *y*-axis represents fold-enrichment relative to IgG controls. $n = 3$ for each group. For (E, G, H and I), data were analyzed using the Student's two-tailed *t*-test. For (F), data analysis was performed using one-way ANOVA with Dunnett's post hoc test. *P < 0.05, **P < 0.01, ***P < 0.001.

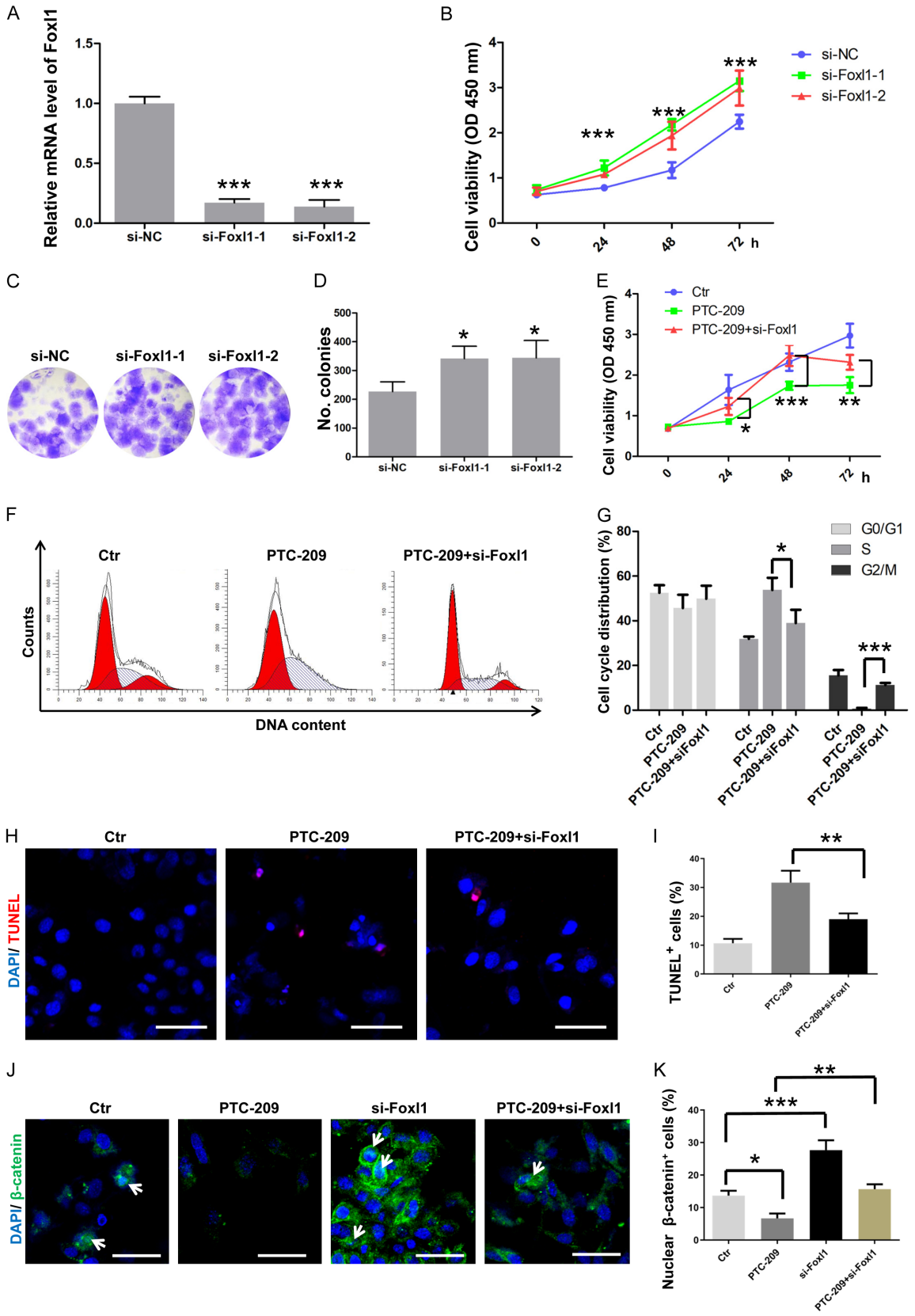


**Figure 3.** *Foxl1* is involved in BMI1-mediated GC-2 cell maintenance. (A) RT-qPCR analysis of *Foxl1* expression in GC-2 cells transfected with negative control (NC) siRNA (si-NC; 50 nM) or siRNAs targeting *Foxl1* (si-*Foxl1*; 50 nM) for 48 h. *n* = 3 for each group. (B) Cell counting kit-8 (CCK-8) assay in GC-2 cells transfected with si-NC or si-*Foxl1*

at the indicated time points. *n* = 6 for each group. (C) Colony formation assay in GC-2 cells transfected with si-NC or si-*Foxl1* for 48 h. *n* = 3 for each group. (D) Quantification of (C). (E) CCK-8 assay in GC-2 cells treated as indicated for 48 h. *n* = 6 for each group. (F) Flow cytometric analysis of the cell cycle in GC-2 cells treated as indicated for 48 h. *n* = 3 for each group. (G) Quantification of (F). (H) TUNEL assay in GC-2 cells treated as indicated for 48 h. *n* = 3 for each group. (I) Quantification of (H). (J) Immunostaining of β-catenin in GC-2 cells treated as indicated for 48 h. *n* = 3 for each group. (K) Percentage of nuclear β-catenin-expressing cells (white arrows) in (J). For (E-K), PTC-209 and si-*Foxl1* were used at the concentrations of 10 μM and 50 nM, respectively. DMSO and si-NC were used as controls (Ctr). Data were analyzed by one-way ANOVA with Dunnett's post hoc test. *P < 0.05, **P < 0.01, ***P < 0.001.

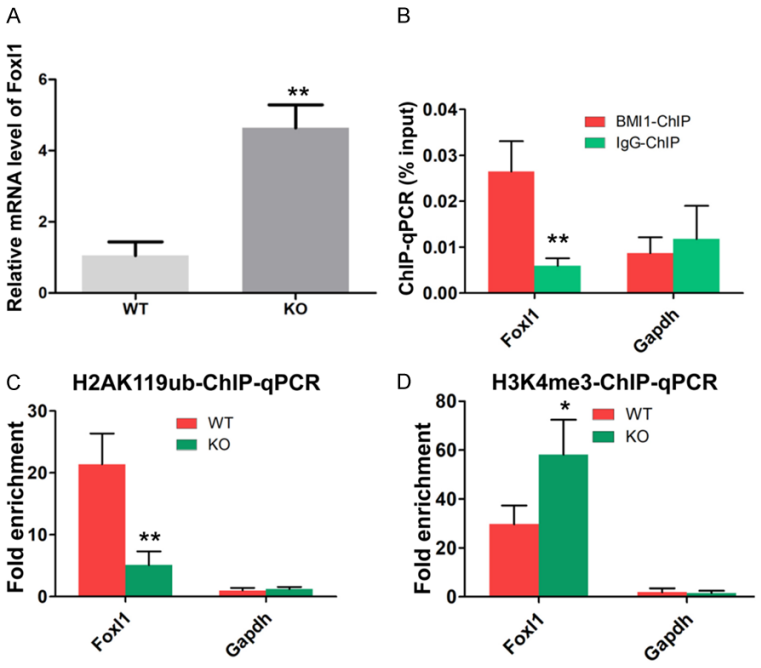


**Figure 4.** BMI1 epigenetically represses *Foxl1* transcription in mouse testes. (A) RT-qPCR analysis of *Foxl1* expression in the testes of wild-type (WT) and *Bmi1*-knockout (KO) mice. (B) ChIP-qPCR of BMI1 distribution in the promoter region of *Foxl1* in mouse testes. (C, D) ChIP-qPCR of H2AK119ub and H3K4me3 distribution in the promoter region of *Foxl1* in the testes of *Bmi1*-WT and *Bmi1*-KO mice. For (A-D), *n* = 3 adult mice per genotype. Data analysis was performed using the Student's two-tailed *t*-test. *P < 0.05, **P < 0.01. WT, wild-type; KO, knockout.

[33]. The translocation of β-catenin to the nucleus is a hallmark of Wnt/β-catenin activation, where it forms a complex with T-cell factor/lymphoid enhancer factor (TCF/LEF) transcription factors and controls the expression of target genes [34, 35]. Studies have revealed that *Foxl1* can negatively regulate Wnt/β-catenin activation in gut epithelia and tumor cells [19, 20]. Accordingly, we examined the distribution of β-catenin in GC-2 cells exposed to PTC-209 treatment, si-*Foxl1*, or both. Immunostaining results showed that PTC-209 treatment, in comparison with the control group, led to a significant reduction in β-catenin expression and nuclear distribution; in contrast, si-Foxl1 therapy resulted in the opposite effect (**Figure 3J** and **3K**). Furthermore, β-catenin expression and distribution were restored in si-*Foxl1* + PTC-209-treated GC-2 cells relative to that seen in cells that only underwent PTC-209 treatment (**Figure 3J** and **3K**). These findings demonstrate that β-catenin signaling is closely linked with the BMI1-*Foxl1* co-regulatory mechanism involved in GC-2 cell survival.

### *BMI1 inhibited Foxl1 expression at the transcriptional level in mice*

Next, we employed *Bmi1*-KO mice to determine whether BMI1 plays a similar role in mouse testes as that observed in GC-2 cells. Foxl1 expression was considerably higher in the testes of Bmi1-KO mice compared to wild-type (WT) animals, which was consistent with the findings in GC-2 cells (**Figure 4A**). It was confirmed by ChIP-qPCR assays that BMI1 was significantly enriched at the Foxl1 promoter region in mouse testes (**Figure 4B**). In comparison to Bmi1-WT mice, H2AK119ub distribution near the Foxl1 promoter area was markedly reduced (**Figure 4C**), whereas that of H3K4me3 was increased in the testes of *Bmi1*-KO mice (**Figure 4D**). Our in vivo and in vitro data showed that BMI1 is crucial for the maintenance of mouse spermatocytes by promoting the assembly of the PRC1 complex and repressing the expression of *Foxl1* (**Figure 5**).

## Discussion

Spermatogenesis is a highly complex process during which unique and extensive chromatin remodeling occurs, resulting in specific epigenetic profiles in spermatozoa [36-38]. Members

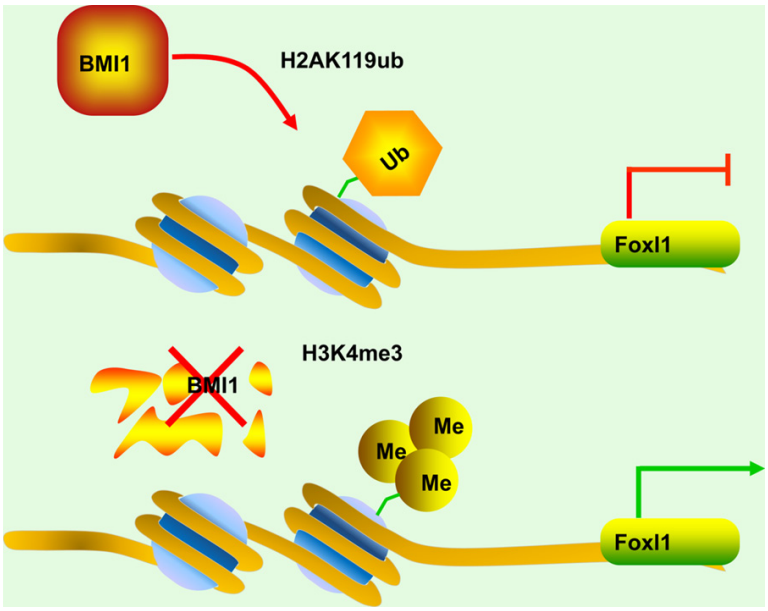


**Figure 5.** Schematic illustration of the working model for the role of BMI1 in GC-2 cells. BMI1 facilitates the monoubiquitination of histone H2A at K119 to repress *Foxl1* expression, thereby maintaining spermatocyte development. In the absence of BMI1, PRC1 function is disrupted and *Foxl1* is transcriptionally activated *via* H3K4me3.

of the PcG protein family are thought to be key in this process, epigenetically mediating the repression of key developmental genes and playing a role in cell proliferation, cell cycle regulation, and apoptosis [39, 40]. Based on biochemical characteristics, members of the PcG protein family can be categorized into two main complexes, namely, PRC2 and PRC1. The former has E3 ubiquitin ligase activity, catalyzing the monoubiquitination of histone H2A lysine 119 (H2AK119ub1) [41, 42]. PRC2, meanwhile, catalyzes the trimethylation of lysine 27 of histone H3 (H3K27me3) [43]. PRC1 has been established in studies to have a significant role in reprogramming the transcriptome during cell proliferation, cell differentiation, and cell cycle progression [44, 45]. For instance, the inactivation of RNF2 (also known as RING1B, the catalytic subunit of PRC1) leads to a gradual loss of spermatogonial stem cell population and meiotic arrest in the mouse testis [44].

We have previously reported that BMI1 is ubiquitously found in all types of testicular cells [9]. BMI1 knockout mice have decreased testosterone production and proliferation of germ cells, likely because of increased oxidative stress and p16/p19 signaling pathway activation [9]. More recently, we also showed that BMI1 accelerates testosterone production in Leydig cells as well as spermatogonia (GC-1 cells) proliferation through epigenetic repression of the p38 MAPK pathway and *Ptprm*, respectively [11, 12]. BMI1's key role in spermatocytes is unclear, in contrast to its involvement in Leydig cells and spermatogonia. In this study, BMI1 controls spermatocyte development via a unique epigenetic route, which we discovered. BMI1-deficient GC-2 cells exhibited compromised viability, cell cycle arrest, and increased rates of cell apoptosis. Mechanistically, we discovered that BMI1 is linked to the Foxl1 promoter region, resulting in the recruitment of PRC1, followed by gene silencing and chromatin remodeling. Importantly, the inhibition of *Foxl1* markedly improved spermatocyte survival in GC-2 cells, which undergo PTC-209-treatment. Moreover, inhibiting BMI1 leads to Foxl1 transcriptional activation and the consequent promotion of β-catenin nuclear translocation in GC-2 cells. Lastly, in Bmi1-KO mice, the connection between BMI1 and Fox11 was confirmed in vivo.

Our *in vivo* and *in vitro* results revealed a role for a BMI1-FOXL1 axis in spermatocytes development in the mouse and gave fresh potential therapeutic targets for male infertility.

## Acknowledgements

This study was funded by National Natural Science Foundation of China (Grant/Award Numbers: 81901532, 81901533, and 3207-1133); Natural Science Foundation of Jiangsu Province (Grant/Award Number: BK201901-88); Suzhou Science and Technology Development Plan (Grant/Award Number: SYSD-2019208); NHC Key Laboratory of Male Reproduction and Genetics (Grant/Award Number: KF201904); Gusu Health Talent Program of Suzhou (Grant/Award Number: GSWS2020068); Open Fund of State Key Laboratory of Reproductive Medicine of Nanjing Medical University (Grant/Award Number:

SKLRMK202010); the Scientific Research Project of Jiangsu Health and Health Committee (Grant/Award Number: Z2021048); and the Open and Shared Research Projects of Large-scale Scientific Research Instruments of Nanjing Medical University (Grant/Award Number: ZC2021DY01).

## Disclosure of conflict of interest

None.

**Address correspondence to:** Bo Zheng, State Key Laboratory of Reproductive Medicine, Center for Reproduction and Genetics, Suzhou Municipal Hospital, The Affiliated Suzhou Hospital of Nanjing Medical University, Gusu School, Nanjing Medical University, Suzhou 215002, Jiangsu, China. Tel: +86-15952038312; E-mail: bozheng@njmu.edu.cn; Yuting Liang, Center for Clinical Laboratory, The First Affiliated Hospital of Soochow University, Suzhou 215006, Jiangsu, China. Tel: +86-158-00572352; E-mail: liangyuting666@126.com; Dan Zhao, Fourth Affiliated Hospital of Jiangsu University, Zhenjiang 212008, Jiangsu, China. Tel: +86-18652885197; E-mail: 624972897@qq.com; Yueshuai Guo, State Key Laboratory of Reproductive Medicine, Department of Histology and Embryology, Nanjing Medical University, Nanjing 211166, Jiangsu, China. Tel: +86-15295751397; E-mail: yueshuai_guo@njmu.edu.cn

## References

[1] Morgan M, Kumar L, Li Y and Baptissart M. Post-transcriptional regulation in spermatogenesis: all RNA pathways lead to healthy sperm. Cell Mol Life Sci 2021; 78: 8049-8071.

[2] Witt E, Benjamin S, Svetec N and Zhao L. Testis single-cell RNA-seq reveals the dynamics of de novo gene transcription and germline mutational bias in drosophila. Elife 2019; 8: e47138.

[3] Zheng B, Zhou Q, Guo Y, Shao B, Zhou T, Wang L, Zhou Z, Sha J, Guo X and Huang X. Establishment of a proteomic profile associated with gonocyte and spermatogonial stem cell maturation and differentiation in neonatal mice. Proteomics 2014; 14: 274-285.

[4] Zhou Q, Guo Y, Zheng B, Shao B, Jiang M, Wang G, Zhou T, Wang L, Zhou Z, Guo X and Huang X. Establishment of a proteome profile and identification of molecular markers for mouse spermatogonial stem cells. J Cell Mol Med 2015; 19: 521-534.

[5] Barbour H, Daou S, Hendzel M and Affar EB. Polycomb group-mediated histone H2A monoubiquitination in epigenome regulation and nuclear processes. Nat Commun 2020; 11: 5947.

[6] Haupt Y, Alexander WS, Barri G, Klinken SP and Adams JM. Novel zinc finger gene implicated as myc collaborator by retrovirally accelerated lymphomagenesis in E mu-myc transgenic mice. Cell 1991; 65: 753-763.

[7] Park IK, Qian D, Kiel M, Becker MW, Pihalja M, Weissman IL, Morrison SJ and Clarke MF. Bmi-1 is required for maintenance of adult self-renewing haematopoietic stem cells. Nature 2003; 423: 302-305.

[8] Park IK, Morrison SJ and Clarke MF. Bmi1, stem cells, and senescence regulation. J Clin Invest 2004; 113: 175-179.

[9] Dai X, Zhang Q, Yu Z, Sun W, Wang R and Miao D. Bmi1 deficient mice exhibit male infertility. Int J Biol Sci 2018; 14: 358-368.

[10] Gao T, Lin M, Shao B, Zhou Q, Wang Y, Chen X, Zhao D, Dai X, Shen C, Cheng H, Yang S, Li H, Zheng B, Zhong X, Yu J, Chen L and Huang X. BMI1 promotes steroidogenesis through maintaining redox homeostasis in mouse MLTC-1 and primary leydig cells. Cell Cycle 2020; 19: 1884-1898.

[11] Yu J, Wu Y, Li H, Zhou H, Shen C, Gao T, Lin M, Dai X, Ou J, Liu M, Huang X, Zheng B and Sun F. BMI1 drives steroidogenesis through epigenetically repressing the p38 MAPK pathway. Front Cell Dev Biol 2021; 9: 665089.

[12] Zhang K, Xu J, Ding Y, Shen C, Lin M, Dai X, Zhou H, Huang X, Xue B and Zheng B. BMI1 promotes spermatogonia proliferation through epigenetic repression of Ptprm. Biochem Biophys Res Commun 2021; 583: 169-177.

[13] Coffer PJ and Burgering BM. Forkhead-box transcription factors and their role in the immune system. Nat Rev Immunol 2004; 4: 889-899.

[14] Perreault N, Sackett SD, Katz JP, Furth EE and Kaestner KH. Foxl1 is a mesenchymal modifier of min in carcinogenesis of stomach and colon. Genes Dev 2005; 19: 311-315.

[15] Qin Y, Gong W, Zhang M, Wang J, Tang Z and Quan Z. Forkhead box L1 is frequently downregulated in gallbladder cancer and inhibits cell growth through apoptosis induction by mitochondrial dysfunction. PLoS One 2014; 9: e102084.

[16] Zhang G, He P, Gaedcke J, Ghadimi BM, Ried T, Yfantis HG, Lee DH, Hanna N, Alexander HR and Hussain SP. FOXL1, a novel candidate tumor suppressor, inhibits tumor aggressiveness and predicts outcome in human pancreatic cancer. Cancer Res 2013; 73: 5416-5425.

[17] Kaestner KH, Silberg DG, Traber PG and Schutz G. The mesenchymal winged helix transcription factor Fkh6 is required for the control of gastrointestinal proliferation and differentiation. Genes Dev 1997; 11: 1583-1595.

[18] Chan AL, La HM, Legrand JMD, Makela JA, Eichenlaub M, De Seram M, Ramialison M and Hobbs RM. Germline stem cell activity is sustained by SALL4-dependent silencing of distinct tumor suppressor genes. Stem Cell Reports 2017; 9: 956-971.
[19] Perreault N, Katz JP, Sackett SD and Kaestner KH. Foxl1 controls the Wnt/beta-catenin pathway by modulating the expression of proteoglycans in the gut. J Biol Chem 2001; 276: 43328-43333.
[20] Wu J, Chen Z, Liu W, Zhang Y, Feng W, Yuan Y, Ye J, Wang L, Cai S, He Y, Wu S and Song W. MicroRNA-188-5p targeting forkhead box L1 promotes colorectal cancer progression via activating Wnt/beta-catenin signaling. Oncol Res 2020; [Epub ahead of print].
[21] Shen C, Zhang K, Yu J, Guo Y, Gao T, Liu Y, Zhang X, Chen X, Yu Y, Cheng H, Zheng A, Li H, Huang X, Ding X and Zheng B. Stromal interaction molecule 1 is required for neonatal testicular development in mice. Biochem Biophys Res Commun 2018; 504: 909-915.
[22] Wu Y, Wang T, Zhao Z, Liu S, Shen C, Li H, Liu M, Zheng B, Yu J and Huang X. Retinoic acid induced protein 14 (Rai14) is dispensable for mouse spermatogenesis. PeerJ 2021; 9: e10847.
[23] Shen Y, Cui X, Hu Y and Zhang Z. LncRNA-MIAT regulates the growth of SHSY5Y cells by regulating the miR-34-5p-SYT1 axis and exerts a neuroprotective effect in a mouse model of Parkinson's disease. Am J Transl Res 2021; 13: 9993-10013.
[24] Wang D, Song X, Zhang N and Guo Y. MiR-1179 represses cell proliferation, migration and invasion of hepatocellular carcinoma through suppression of NUAK2. Am J Transl Res 2022; 14: 223-239.
[25] Xu Z, Xu L, Ge Y, Sun H, Zhu J, Dou Q and Jia R. Cabazitaxel suppresses the proliferation and promotes the apoptosis and radiosensitivity of castration-resistant prostate cancer cells by inhibiting PI3K/AKT pathway. Am J Transl Res 2022; 14: 166-181.
[26] Liu Y, Yu X, Huang A, Zhang X, Wang Y, Geng W, Xu R, Li S, He H, Zheng B, Chen G and Xu Y. INTS7-ABCD3 interaction stimulates the proliferation and osteoblastic differentiation of mouse bone marrow mesenchymal stem cells by suppressing oxidative stress. Front Physiol 2021; 12: 758607.
[27] Jia L, Zhang W and Wang CY. BMI1 inhibition eliminates residual cancer stem cells after PD1 blockade and activates antitumor immunity to prevent metastasis and relapse. Cell Stem Cell 2020; 27: 238-253.
[28] Zhu S, Zhao D, Li C, Li Q, Jiang W, Liu Q, Wang R, Fazli L, Li Y, Zhang L, Yi Y, Meng Q, Wang W, Wang G, Zhang M, Zu X, Zhao W, Deng T, Yu J, Dong X, Chen K and Cao Q. BMI1 is directly regulated by androgen receptor to promote castration-resistance in prostate cancer. Oncogene 2020; 39: 17-29.
[29] Wang Q, Wu Y, Lin M, Wang G, Liu J, Xie M, Zheng B, Shen C and Shen J. BMI1 promotes osteosarcoma proliferation and metastasis by repressing the transcription of SIK1. Cancer Cell Int 2022; 22: 136.
[30] Zhou Y, Wang L, Vaseghi HR, Liu Z, Lu R, Alimohamadi S, Yin C, Fu JD, Wang GG, Liu J and Qian L. Bmi1 is a key epigenetic barrier to direct cardiac reprogramming. Cell Stem Cell 2016; 18: 382-395.
[31] Hasegawa K, Sin HS, Maezawa S, Broering TJ, Kartashov AV, Alavattam KG, Ichijima Y, Zhang F, Bacon WC, Greis KD, Andreassen PR, Barski A and Namekawa SH. SCML2 establishes the male germline epigenome through regulation of histone H2A ubiquitination. Dev Cell 2015; 32: 574-588.
[32] Benayoun BA, Pollina EA, Ucar D, Mahmoudi S, Karra K, Wong ED, Devarajan K, Daugherty AC, Kundaje AB, Mancini E, Hitz BC, Gupta R, Rando TA, Baker JC, Snyder MP, Cherry JM and Brunet A. H3K4me3 breadth is linked to cell identity and transcriptional consistency. Cell 2014; 158: 673-688.
[33] Clevers H and Nusse R. Wnt/beta-catenin signaling and disease. Cell 2012; 149: 1192-1205.
[34] Zheng B, Yu J, Guo Y, Gao T, Shen C, Zhang X, Li H and Huang X. Cellular nucleic acid-binding protein is vital to testis development and spermatogenesis in mice. Reproduction 2018; 156: 59-69.
[35] Angers S and Moon RT. Proximal events in Wnt signal transduction. Nat Rev Mol Cell Biol 2009; 10: 468-477.
[36] Lismer A, Siklenka K, Lafleur C, Dumeaux V and Kimmins S. Sperm histone H3 lysine 4 trimethylation is altered in a genetic mouse model of transgenerational epigenetic inheritance. Nucleic Acids Res 2020; 48: 11380-11393.
[37] Aston KI, Uren PJ, Jenkins TG, Horsager A, Cairns BR, Smith AD and Carrell DT. Aberrant sperm DNA methylation predicts male fertility status and embryo quality. Fertil Steril 2015; 104: 1388-1397.
[38] Katz DJ, Edwards TM, Reinke V and Kelly WG. A C. elegans LSD1 demethylase contributes to germline immortality by reprogramming epigenetic memory. Cell 2009; 137: 308-320.
[39] Pasini D, Bracken AP, Jensen MR, Lazzerini Denchi E and Helin K. Suz12 is essential for mouse development and for EZH2 histone methyltransferase activity. EMBO J 2004; 23: 4061-4071.

[40] Schuettengruber B, Bourbon HM, Di Croce L and Cavalli G. Genome regulation by polycomb and trithorax: 70 years and counting. Cell 2017; 171: 34-57.
[41] de Napoles M, Mermoud JE, Wakao R, Tang YA, Endoh M, Appanah R, Nesterova TB, Silva J, Otte AP, Vidal M, Koseki H and Brockdorff N. Polycomb group proteins Ring1A/B link ubiquitylation of histone H2A to heritable gene silencing and X inactivation. Dev Cell 2004; 7: 663-676.
[42] Buchwald G, van der Stoop P, Weichenrieder O, Perrakis A, van Lohuizen M and Sixma TK. Structure and E3-ligase activity of the Ring-Ring complex of polycomb proteins Bmi1 and Ring1b. EMBO J 2006; 25: 2465-2474.
[43] Blackledge NP and Klose RJ. Getting under the skin of polycomb-dependent gene regulation. Genes Dev 2021; 35: 301-303.
[44] Maezawa S, Hasegawa K, Yukawa M, Sakashita A, Alavattam KG, Andreassen PR, Vidal M, Koseki H, Barski A and Namekawa SH. Polycomb directs timely activation of germline genes in spermatogenesis. Genes Dev 2017; 31: 1693-1703.
[45] Spaapen F, van den Akker GG, Caron MM, Prickaerts P, Rofel C, Dahlmans VE, Surtel DA, Paulis Y, Schweizer F, Welting TJ, Eijssen LM and Voncken JW. The immediate early gene product EGR1 and polycomb group proteins interact in epigenetic programming during chondrogenesis. PLoS One 2013; 8: e58083.

**Table S1.** Putative interactors identified in this study

| Majority protein IDs | Full protein names | Protein names | Unique peptides-BMI1 | Unique peptides-IgG | Sequence coverage [%] | Mol. weight [kDa] | Sequence length |
|---|---|---|---|---|---|---|---|
| Q9CQJ4 | E3 ubiquitin-protein ligase RING2 | Rnf2 | 8 | 0 | 31 | 37.623 | 336 |
| Q9QXV1 | Chromobox protein homolog 8 | Cbx8 | 7 | 0 | 21.3 | 39.859 | 362 |
| P25916 | Polycomb complex protein BMI-1 | Bmi1 | 6 | 0 | 27.5 | 36.707 | 324 |
| O35730 | E3 ubiquitin-protein ligase RING1A | Ring1A | 6 | 0 | 24.1 | 42.63 | 406 |
| Q9QWH1 | Polyhomeotic-like protein 2 | Phc2 | 4 | 0 | 8.7 | 35.747 | 323 |
| E9Q557 | Desmoplakin | Dsp | 4 | 0 | 1.3 | 332.91 | 2883 |
| F8WHN2 | Chromobox protein homolog 7 | Cbx7 | 2 | 0 | 8.4 | 28.625 | 251 |
| Q02257 | Junction plakoglobin | Jup | 2 | 0 | 3.2 | 81.8 | 745 |
| P08113 | Endoplasmin | Hsp90b1 | 2 | 0 | 4.6 | 92.475 | 802 |
| A0A0J9YU29 | Zinc finger protein 512 | Znf512 | 1 | 0 | 20.8 | 8.5748 | 72 |
| O55112 | AF4/FMR2 family member 2 | Aff2 | 1 | 0 | 0.9 | 140.18 | 1272 |
| H3BLB8 | Serum paraoxonase/arylesterase 1 | Pon1 | 1 | 0 | 7.7 | 20.222 | 181 |
| A8C756-3 | Thyroid adenoma-associated protein homolog | Thada | 1 | 0 | 2 | 56.646 | 500 |
| Q99LC5 | Electron transfer flavoprotein subunit alpha | Etfa | 1 | 0 | 5.7 | 35.009 | 333 |
| Q02105 | Complement C1q subcomponent subunit C | C1qc | 1 | 0 | 4.1 | 25.991 | 246 |
| A0A087WP98 | Prothymosin alpha | Ptma | 1 | 0 | 24.1 | 6.4913 | 58 |
| P61965 | WD repeat-containing protein 5 | Wdr5 | 1 | 0 | 3.9 | 36.588 | 334 |
| P68510 | 14-3-3 protein eta | Ywhah | 1 | 0 | 6.9 | 28.211 | 246 |
| D3YY55 | Sin3A associated protein 18 | Sap18 | 1 | 0 | 11.2 | 12.485 | 107 |
| Q8BHE0 | Proline-rich protein 11 | Prr11 | 1 | 0 | 3.3 | 40.948 | 368 |
| A0A0U1RP90 | Protein LSM14 homolog A | Lsm14a | 1 | 0 | 6.3 | 17.12 | 158 |
| P11438 | Lysosome-associated membrane glycoprotein 1 | Lamp1 | 1 | 0 | 2.7 | 43.865 | 406 |
| P30658 | Chromobox protein homolog 2 | Cbx2 | 1 | 0 | 3.5 | 54.917 | 519 |
| O70435 | Proteasome subunit alpha type-3 | Psma3 | 1 | 0 | 4.7 | 28.405 | 255 |
| P63085 | Mitogen-activated protein kinase 1 | Mapk1 | 1 | 0 | 3.4 | 41.275 | 358 |
| D3Z0U5 | Katanin p60 ATPase-containing subunit A-like 2 | Katnal2 | 1 | 0 | 4.3 | 31.2 | 277 |
| A0A2R8VHX5 | Zinc finger protein 385A | Znf385a | 1 | 0 | 2.6 | 36.28 | 347 |